3.36 High-temperature Hydrogen Attack

3.36.1 Description of Damage

a) High-temperature hydrogen attack (HTHA) results from exposure of steels to hydrogen gas at elevated temperatures and pressures. Dissociated hydrogen atoms react with carbon and carbides in the steel to form CH_4.

b) The hydrogen/carbon reaction can cause surface decarburization of the steel. Surface decarburization alone is normally not detrimental to the point of limiting the life of equipment but may be indicative of internal HTHA. Extensive decarburization will reduce component strength. (See 3.25 for more on decarburization.)

c) If diffusion of carbon to the surface is limited, CH_4 is formed internally from internal decarburization. Internal CH_4 cannot diffuse through the steel. As a result, internal CH_4 pressure builds up, initially forming bubbles or cavities, then microfissures, and finally fissures that may combine to form cracks. Internal damage leading to cracking is the more serious effect of HTHA, and it can lead to equipment failure.

d) Failure can occur when the cracks reduce the load (pressure) carrying ability of the pressure-containing part.

e) Blistering may also occur due to either molecular hydrogen (from re-combined hydrogen atoms) or CH_4 accumulating in laminations or other conducive sites in the steel.

f) See Reference 1 (API RP 941) for more detailed information on HTHA.

3.36.2 Affected Materials

a) In order of increasing resistance: as-welded (non-PWHT) carbon steel, non-welded carbon steel and carbon steel that has received PWHT, C-0.5Mo, Mn-0.5Mo, 1Cr-0.5Mo, 1.25Cr-0.5Mo, 2.25Cr-1Mo, 2.25Cr-1Mo-V, 3Cr-1Mo, 5Cr-0.5Mo, and similar steels with variations in chemistry.

b) 300 series SS, as well as 5Cr, 9Cr, and 12Cr alloys, are not susceptible to HTHA at conditions normally seen in refinery units.

3.36.3 Critical Factors

a) Resistance to HTHA increases with an increase in the alloy content, primarily the Cr and Mo content, of a steel. For a specific material, HTHA is dependent on temperature, hydrogen partial pressure, time, and stress level.

b) Figure 3-36-1, from API RP 941, is a set of curves that show the combined temperature and hydrogen partial pressure safe operating limits for carbon steel and low-alloy steels. Operation at a temperature and H_2 partial pressure below the curve for a particular material is considered safe. Operation above the curve indicates susceptibility to HTHA. Additional information on HTHA can be found in API RP 941.

c) HTHA damage is preceded by a period of time when no noticeable change in properties is detectable by normal mechanical testing techniques nor is any internal damage detectable with any NDE methods. This period of time is called the incubation period.

   1. During the incubation period, the amount of internal damage (cavity and microfissure formation and growth) increases to the point where it can be detected and measured with available inspection techniques. It may vary from hours under very severe conditions to many years.

d) The damage is irreversible, and service exposure time is cumulative. After the incubation period, the amount of damage continues to increase during the time the material is exposed to damaging temperature and H_2 partial pressure conditions, whether the exposure is continuous or periodic.

e) Applied or residual tensile stress can increase the rate of HTHA damage occurring in a susceptible material. Stress-relieving carbon steel welds by PWHT is known to reduce susceptibility to HTHA.

3.36.4 Affected Units

a) Hydroprocessing units such as hydrotreaters (desulfurizers) and hydrocrackers, catalytic reformers, some ISOM units, hydrogen manufacturing units, and hydrogen cleanup units such as pressure swing absorption units all have equipment operating under conditions where HTHA can occur in a susceptible material.

b) Boiler tubes in very high pressure steam service can also suffer HTHA.

3.36.5 Appearance or Morphology of Damage

a) The location within a piece of equipment where HTHA will occur is generally unpredictable. HTHA that led to equipment failure or replacement has occurred in weld HAZs as well as base metal away from welds. It is less commonly found in weld metal.

b) HTHA can be confirmed through the use of specialized techniques including metallographic and SEM analysis of damaged areas. (Figure 3-36-2 to Figure 3-36-6)

c) The steel surface may be decarburized. (Figure 3-36-4)

d) Internal decarburization can lead to internal fissuring and cracking, which in the later stages of damage can be seen using standard metallography. (Figure 3-36-5 to Figure 3-36-6)

e) In the earliest stages of HTHA, bubbles/cavities in samples can be detected by SEM, although it may be difficult to tell the difference between HTHA cavities and creep cavities. (Some refinery services expose low-alloy steels to both HTHA and creep conditions.) Advanced metallographic analysis of damaged areas can detect the early stages of microfissuring.

f) Cracking and fissuring are intergranular and occur adjacent to pearlite (layers of ferrite and iron carbide) areas in carbon steels.

g) Cracking along the HAZ and fusion line can occur in carbon steel as the result of highly localized HTHA, with adjacent areas exhibiting little or no fissuring or decarburization

h) Blistering may be visible to the naked eye.

3.36.6 Prevention/Mitigation

a) Using alloy steels with chromium and molybdenum will increase carbide stability, thereby minimizing CH_4 formation and resistance to HTHA. Other carbide stabilizing elements include tungsten and vanadium.

b) Common design practice is to use a 25 °F to 50 °F (15 °C to 30 °C) and 25 psia to 50 psia (170 KPa to 345 KPa) hydrogen partial pressure safety factor approach when using the API RP 941 curves.

c) The API RP 941 curves, with the current version shown in Figure 3-36-1, have been revised several times since they were first introduced.

   1. The C-½Mo curve was removed from Figure 3-36-1 in 1990 because of a number of cases of HTHA in C-½Mo steels in refinery service under conditions that were previously considered safe, i.e. below the previously existing C-½Mo curve. This material is not recommended for new construction in hot hydrogen services. (C-½Mo carbide stability under HTHA conditions is variable due to the different carbides formed during the various heat treatments applied to fabricated equipment.)

d) For existing C-½Mo equipment, the concern about its unpredictable resistance to HTHA has prompted refiners to perform reviews of inspection effectiveness and cost vs replacement with a more suitable alloy.

   1. Non-stress-relieved carbon steel welds have also shown a higher susceptibility to HTHA compared to stress-relieved welds and non-welded components. In response, the Eighth Edition of API RP 941 added a new, lower curve for carbon steel welded with no PWHT, as shown in Figure 3-36-1.

e) 300 series SS weld overlay and roll bond cladding, and in some cases 400 series SS cladding, are typically used in high-temperature hydrogen service where the base metal does not have adequate high-temperature H_2/H_2S corrosion resistance. Properly metallurgically bonded stainless steel overlay or cladding will decrease the hydrogen partial pressure seen by the underlying base metal; however, most refiners do not take credit for this in the design of new equipment. New equipment should be designed so the base material is inherently resistant to HTHA under expected service conditions without taking into account any added HTHA resistance provided by the weld overlay or cladding.

1. In some cases, refiners take the decrease in effective partial pressure into account when evaluating the risk of HTHA in existing equipment.

3.36.7 Inspection and Monitoring

a) Damage may occur randomly in the base metal, weld HAZs, and occasionally in welds.

b) HTHA can occur in the base metal at locations remote from welds. In vessels with internal cladding or weld overlay, HTHA damage can occur in the base metal at locations where the cladding or weld overlay has cracked and become disbonded, especially if credit was taken for the cladding reducing the effective H_2 partial pressure at the base metal, i.e. where the vessel's operating conditions exceeded the API RP 941 curve for unprotected base metal. PT of the cladding or weld overlay for cracking can assist in identifying areas that may have HTHA damage in the base metal underneath the cracked cladding or weld overlay.

1. VT for bulging of the cladding or weld overlay away from the underlying base metal may also aid in identifying suspect areas of HTHA damage in the base metal.

2. Localized damage under cladding or weld overlay might be overlooked if inspection methods focus only on the weld seams and nozzles. (Reference 4)

c) While FMR can detect microvoids, fissures, and decarburization, it is best suited for examination in areas of known HTHA damage and is generally not relied upon as the primary tool for damage detection. Most equipment has decarburized surfaces due to the various heat treatments used during fabrication, and microvoids and fissures may also be absent on the surface. Experience has shown that removal of metal up to 0.1 in. (2 mm) may be needed for finding HTHA damage.

d) VT for blisters on the inside surface may indicate CH_4 formation and potential HTHA. However, HTHA mostly occurs without the formation of surface blisters.

e) The use of NDE methods to detect internal HTHA requires highly specialized training, skills, and experience. It has had mixed results and is an area of ongoing development. As of this writing, the NDE table in API RP 941 is undergoing revision.

1. Automated ultrasonic backscatter testing (AUBT) and angle beam spectral analysis (ABSA) have had some success finding fissuring, i.e. where microvoids and microfissures have grown to form significant fissures in the base metal as well as in welds and HAZs, but it can also miss significant cracking and is not considered reliable.

2. TOFD and PAUT have shown promise in finding surface-connected and internal damage.

3. Conventional NDE methods for crack detection, e.g. WFMT, PT, or MT, are generally not useful for HTHA inspection except where gross cracking has occurred and reached the metal surface.

4. AET is not a proven method for the detection of damage.

5. Ultrasonic attenuation and velocity ratio have been found to be unreliable techniques for HTHA detection and should not be used as primary inspection methods.

3.36.8 Related Mechanisms

Decarburization (3.25). A form of HTHA can occur in boiler tubes and is referred to by the fossil utility industry as hydrogen damage.

3.36.9 References

1. API Recommended Practice 941, *Steels for Hydrogen Service at Elevated Temperatures and Pressures in Petroleum Refineries and Petrochemical Plants*, 8th Edition, American Petroleum Institute, Washington, DC

2. F.H. Vitovec et al., "The Growth Rate of Fissures During Hydrogen Attack of Steels," *Proceedings of the API Division of Refining*, Vol. 44, No. 3, 1964, pp. 179–188.

3. "Fitness-For-Service Evaluation Procedures for Operating Pressure Vessels, Tanks, and Piping in Refinery and Chemical Service," Materials Properties Council, FS-26, Draft No. 5, Consultants Report, NY, 1995.

4. S. Decker et al., "Safe Operation of a High Temperature Hydrogen Attack Affected DHT Reactor," Paper No. 09339, *Corrosion/2009*, NACE International, Houston, TX.

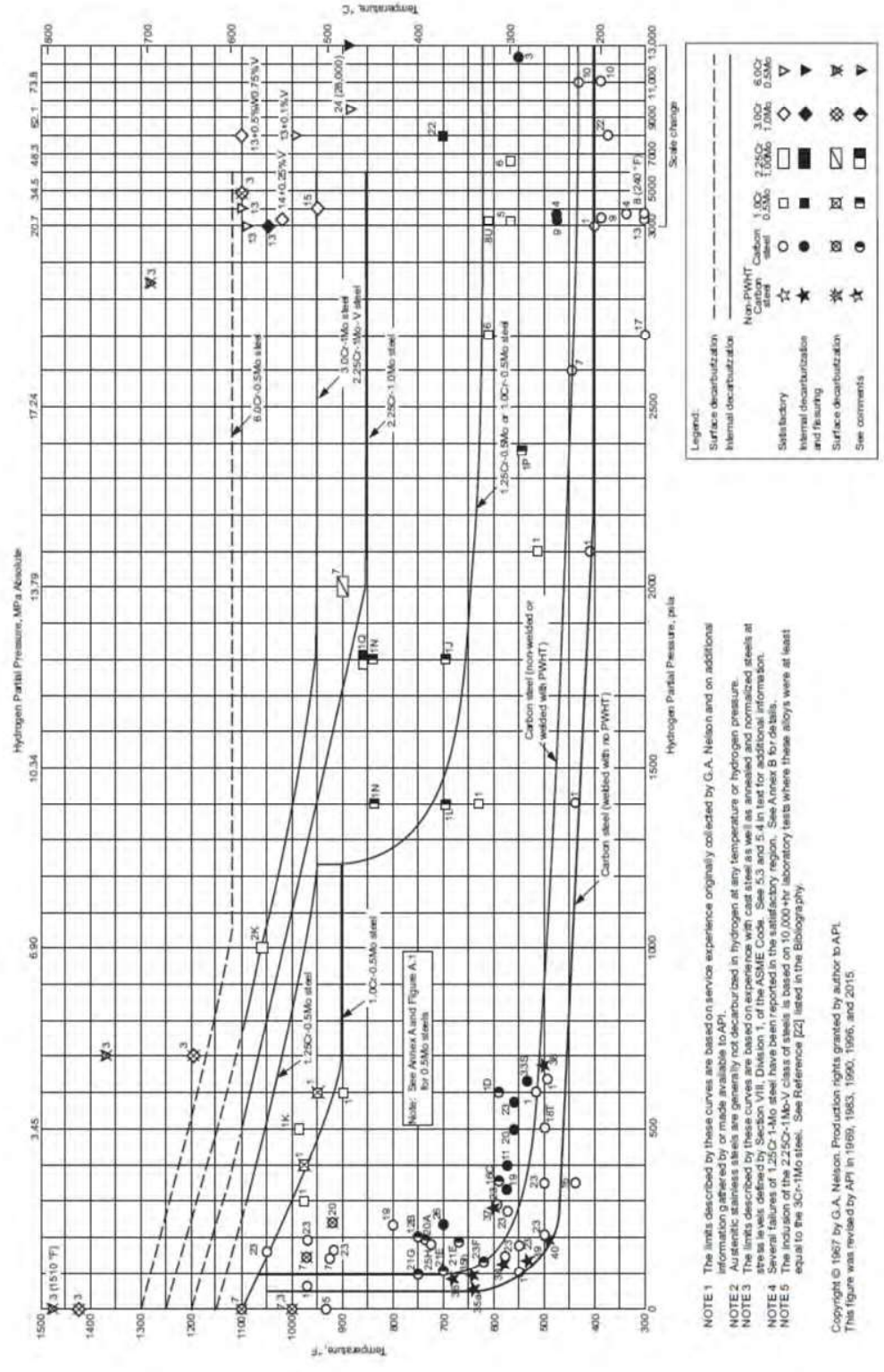

Figure 3-36-1—Recommended temperature and H_2 partial pressure limits per API RP 941. (Reference 1)

Figure 3-36-2—A pair of 10-in. C-½Mo flanged pipe sections (SA335-P1 and SA234-WP1) from a hot bypass line in a catalytic reformer that was designed to remain closed but operated partially or fully open for unknown lengths of time. They were in service for ~34 years at temperatures up to 960 °F (515 °C) with a hydrogen partial pressure of 198 psig (1.4 MPa).

Figure 3-36-3—A photomicrograph of the OD surface of a pipe section from Figure 3-35-2 exhibits a normal ferritic-pearlitic microstructure. Magnification 200X.

Figure 3-36-4—A photomicrograph at the ID surface of the pipe in Figure 3-35-2 shows complete decarburization of the original structure. Magnification 200X.

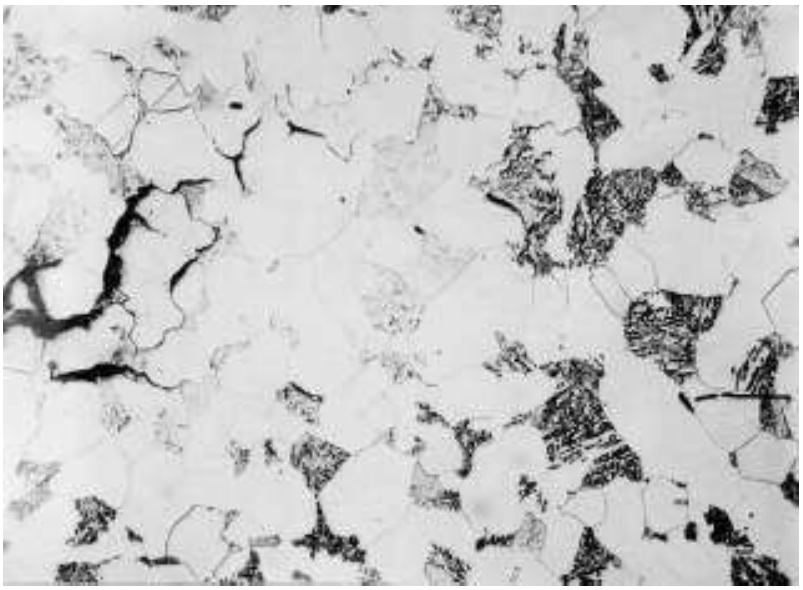

Figure 3-36-5—A photomicrograph illustrating internal decarburization and fissuring of C-½Mo steel.

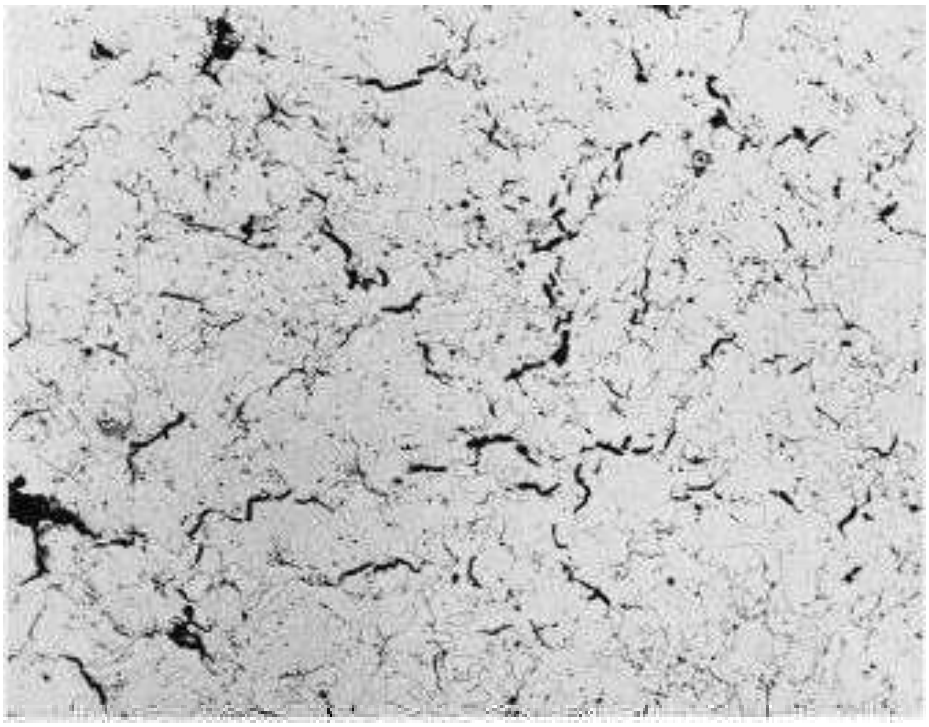

Figure 3-36-6—A high-magnification photomicrograph showing linkup of microfissures to form continuous cracks. Note that damage is accompanied by a significant amount of internal decarburization.